Journal of Quality Engineering and Production Optimization

Volume 9, Issue 2, Summer & Autumn 2024

http://jqepo.shahed.ac.ir

Research Paper

DOI: 10.22070/jqepo.2025.18419.1271

Simultaneous monitoring of time between events and their multivariate magnitude

Mohammadreza Mirzaei Novin [1], Amirhossein Amiri [1*]

[1] *Department of Industrial Engineering, Faculty of Engineering, Shahed University, Tehran, Iran*

**** Corresponding Author:** Amirhossein Amiri (Email: amiri@shahed.ac.ir)*

Abstract *– Monitoring the time between events without accounting for their magnitudes is an impractical approach. This paper discusses the monitoring of the time between events (TBEs) and their multivariate magnitude (M). The paper explores control charts for the magnitude of events in a multivariate setting, focusing on situations where the magnitude of events has two dimensions. Two statistics are presented for the simultaneous monitoring of the time between events and the multivariate magnitude. The first statistic is a standardized EWMAZ, based on the Shewhart-EWMA approach. The second statistic is a set of three standardized single EWMAs, each used for monitoring TBEs and the two dimensions of magnitude (TSEWMA). The performance of these statistics is evaluated by considering different shifts in the mean of TBE and magnitude under three distinct shift parameter values. The results confirm their effectiveness across various conditions.*

Keywords*– High-quality process, Statistical process monitoring (SPM), Time between events, Time between events and magnitude, Average run length (ARL).*

I. INTRODUCTION

Techniques of statistical quality control play a crucial role across various manufacturing and service sectors. These methods encompass acceptance sampling, statistical process monitoring (SPM), experimental design, and process capability analysis. Within these approaches, control charts serve as essential instruments in SPM. One notable type is the Time Between Events (TBE) control chart, utilized specifically for monitoring processes characterized by high quality and infrequent occurrences.

In this context, “time” refers to the duration between two consecutive events. These events can be categorized as either positive or negative. Examples of positive events include receiving orders, observing animal species in natural ecosystems, and capital returns. Negative events include product non-compliance during production, natural disasters like fires and earthquakes, cyber-attacks, and nuclear reactor failures.

Control charts are a fundamental tool for monitoring high-quality processes, and their traditional forms have been thoroughly studied by Xie et al. (2002). Calvin (1983) was the first to introduce a control chart for

Manuscript Received: 5-May-2024 & Revised:17-July-2024 & Accepted: 11-September-2024
ISSN: 2423-3781

high-quality processes, which was based on process geometry. Lucas (1985) and Vardeman and Ray (1985) were the trailblazers in proposing the Time Between Events (TBE) control charts for monitoring high-quality processes. Goh (1987) carried out a study on the geometric chart's properties and coined it the Cumulative Compliance Control Chart (*CCC*). Di Bucchianico et al. (2005) utilized *CCC-r*, a generalization of the geometric chart based on the negative binomial distribution, in their study of a high-volume coffee packing plant. Albers and Kallenberg (2006) put forth a nonparametric iteration of the negative binomial distribution for the surveillance of high-quality processes. He et al. (2006) presented a control chart based on the generalized Poisson distribution to monitor over-dispersed time-between-events data. Wu et al. (2009a) introduced the np_x chart, which combines descriptive inspection and increased design sensitivity by incorporating warning limits with past control limits. Chen and Chen (2012) enhanced the power of the *CCC* chart by extending it to *VSS* for geometric processes. He et al. (2012) introduced the *Omega-Event* Counted chart (CBΩ), defining an omega as an event falling within a specified interval. Qu et al. (2014) employed sequential analysis and discontinuity techniques to construct control charts. Aslam et al. (2014) introduced an exponential TBE control chart based on repeated sampling using warning limits and performance limits. Maleki et al. (2016) used a simultaneous monitoring approach to monitor the mean and variance. In their study, they investigated the impact of measurement error with linearly increasing variance on the performance of the ELR control chart for simultaneous monitoring of the multivariate process mean vector and covariance matrix. Amiri et al. (2018) investigated the simultaneous monitoring of multivariate linear regression profiles and the generalized linear model (GLM) in Phase II. Since independently monitoring these profiles may lead to inaccurate results, this research proposes methodologies for simultaneous monitoring. The effectiveness of the proposed approaches is assessed through simulation studies, which demonstrate their superior performance compared to separate monitoring techniques. Ali et al. (2020) conducted an investigation on the *CCC* chart, assuming a discrete Weibull distribution, within the context of a reliability study. Abubakar et al. (2021) developed a control chart that employed variable sampling intervals and the EWMA-CCC to monitor the cumulative count of inspected items until a non-conformity was detected. Dogu and Noor-ul-amine (2021) discussed the design of a self-initiated EWMA control chart for TBE data following an exponential distribution. Hu et al. (2021) implemented an adaptive EWMA chart to monitor time-between-events data that follows a gamma distribution. It is crucial to note that the choice of monitoring tools depends on data conditions and their complexity. As data dimensions and complexity evolve, the need for suitable control tools also changes accordingly. Therefore, charts that are suitable for monitoring univariate quality characteristics may not be applicable for multivariate ones.

Kumar et al. (2024) introduced ATS-unbiased control charts tailored for high-rate manufacturing processes with rare defects, replacing the traditional ARL metric with ATS to better handle unequal inter-event times and enhance out-of-control detection. Their approach, based on exponential inter-event times and gamma-distributed cumulative event times, employs chi-square-based control limits and integrates run rules to improve early shift detection. Guo et al. (2024) developed an optimized TBE control chart designed for exponentially distributed inter-event times, addressing parameter estimation challenges in Phase I data. By minimizing SDARL, their model stabilizes performance while ensuring effective shift detection, demonstrating superior accuracy in real-world applications, such as coal mining incidents and volcanic earthquakes. Hu et al. (2024) proposed a hybrid Shewhart-EWMA-CUSUM chart, combining memory-based and memoryless control charts to enhance the detection of both minor and major process shifts in high-quality systems with low defect rates. Evaluated using LED failure data, this approach outperforms individual Shewhart, EWMA, and CUSUM charts. Niaz et al. (2025) introduced a modified one-sided EWMA_MP control chart, incorporating power transformations and a two-level optimization model to enhance sensitivity to both upward and downward shifts in exponentially distributed TBE data. Their model optimally adjusts parameters to minimize EARL and EWRL, improving detection accuracy and process monitoring efficiency compared to existing methods.

Zwetsloot et al. (2020) performed a comprehensive analysis on multivariate time between events, examining two different scenarios. Their study highlighted that although monitoring the interval between events is crucial, integrating the magnitude of events can significantly improve process surveillance. For instance, in the case of natural fires, it is essential not only to monitor the intervals between occurrences but also to account for factors such as the burned area and the related economic impacts. Wu et al. (2009b) introduced control charts capable of simultaneously tracking both

the time between events and their magnitudes, without explicitly relying on the assumption of a Poisson distribution. Similarly, Sanusi et al. (2020) utilized the EWMAZ control chart to investigate the concurrent monitoring of event magnitudes and the intervals between them. Rahali et al. (2019) performed a comparative analysis of existing control charts in the literature, emphasizing simultaneous monitoring of the time between events and their magnitudes by employing multiple distributions (Gamma, Weibull, Log-normal, and Normal) alongside three standardized statistics. In a separate study, Rahali et al. (2021) examined the correlation between the magnitude of events and the intervals between them, employing the same three statistics mentioned earlier. Ali (2021) conducted research on control charts designed for the simultaneous monitoring of magnitude and time, under the assumption of a power law process governing the intervals between events, and considered both cumulative and non-cumulative magnitudes. Shamstabar et al. (2021) directed their study toward the reliability monitoring of systems subject to deterioration processes driven by cumulative shocks. Amjadi and Sabri-Laqaei (2022) proposed a median-rate control chart designed for simultaneously monitoring both the magnitude of events and the time intervals between occurrences. Janada et al. (2022) introduced a new control chart design capable of tracking multi-state systems, representing an innovative approach to probability-limit control charts. Their study illustrated that it is feasible to monitor state transitions both individually and concurrently.

The quality of a process is determined by several critical factors that collectively define a multivariate process. In their research, Hakimia et al. (2022) applied two novel control charts to monitor subscriber consumption. These multivariate ordinal charts, known as the MR chart and the Multivariate Ordinal Categorical (MOC) chart, were used for process monitoring in Phase II, utilizing the ordinal log-linear model. Chen and Chiuo (2023) proposed an innovative condition-based maintenance (CBM) model using an X/T control chart to monitor the frequency and severity of facility failures simultaneously in a simple repairable queuing system. Pu and Li (2023) proposed the spatiotemporal Epidemic-Type Aftershock Sequence (ETAS) model with the aim of simulating regional aftershock sequences. They also established a framework to assess the probability of structural failure caused by aftershocks. Mirzaei Novin and Amiri (2023) utilized a multivariate marked Hawkes process to model the multivariate time between events and the magnitude of events. They then proposed three statistics for simultaneous monitoring of the time between events and the corresponding magnitudes. Zwetsloot et al. (2023) proposed a bivariate Time-Between-Events (TBE) control chart for the early detection of changes in event frequency across various fields. Unlike existing methods, this chart provides real-time signals, thereby enhancing detection ability, particularly for processes with varying rates. The method, supported by analytical expressions for control limits, outperforms existing ones and has been tested on real-life datasets. Talib et al. (2024) proposed a Max-EWMA control chart, assuming a generalized exponential distribution for both time and magnitude, and demonstrated the application of the proposed method in a real-world case study. The existing literature encompasses a variety of conditions, including multivariate time between events and different modes of magnitude. However, this study distinguishes itself by considering multivariable situations that involve conflicting magnitudes across multiple components. In many scenarios, monitoring only the time between events is insufficient.

In such cases, considering the magnitude of events with their multiple dimensions is essential for a comprehensive analysis. This research aims to highlight the importance of monitoring high-quality processes in scenarios where event magnitudes involve multiple components. While control charts have been previously devised to monitor multi-component processes, no study has yet explored the conditions for concurrently monitoring the time between events and magnitude, such that the magnitude of events adheres to a distribution with more than one component. For instance, in a critical component failure analysis, it is essential to monitor the time between failures in conjunction with repair and obsolescence costs. Similarly, in the context of fires, it is crucial to monitor the time between fires along with factors such as the extent of the fire and associated costs.

This study proposes two statistical methods for the simultaneous monitoring of time between events and event magnitudes: (1) the Standardized EWMAZ statistic, and (2) the TSEWMA statistic, which comprises three standardized individual EWMA statistics designed to monitor the time between events along with the two dimensions of magnitude.

The structure of the paper is organized as follows: Section II focuses on modeling the time between events and

multivariate magnitudes. Section III introduces the Standardized EWMAZ statistic alongside the three standardized single EWMA statistics for monitoring both the time between events and magnitudes. Section IV provides a comparative analysis of the proposed statistics through a numerical example. Section V presents a detailed comparison study to highlight the advantages of the proposed control charts over existing methods in the literature. Finally, the concluding section summarizes the findings and outlines recommendations for future research.

II. MODELING TBEs AND MULTIVARIATE MAGNITUDE

As previously discussed, events can be categorized as either positive or negative. A positive event is desirable within a short time frame; therefore, a shorter interval between these events indicates a more favorable outcome. Conversely, a negative event is undesirable, and a longer interval between occurrences is preferable. This study focuses on the latter, aiming to quickly detect any reduction in the time between occurrences.

To further illustrate this, consider a scenario in which firefighting services are deployed to extinguish fires in a large city containing various facilities, such as an amusement park, a museum, and fuel storage tanks. If the time between fires is considered as the time between events and the magnitude of each fire is represented by two dimensions—namely, the cost ($) and the extent (square meters)—then the events can be categorized as follows:

1. High-cost fires with a small size.
2. High-cost fires with a large size.
3. Low-cost fires with a large size.
4. Low-cost fires with a small size.

Fig. 1 provides an illustration of ten fires. The horizontal axis denotes the count of fires, while the vertical axis represents the magnitude (cost in thousands of dollars and extent in square meters). The objectives of monitoring these parameters are as follows:

1. Detecting Out-of-Control Conditions: This involves identifying out-of-control conditions in the time between fires, which could indicate vandalism, natural environmental causes, or seasonal factors.
2. Early Detection of Out-of-Control Processes: This pertains to the early detection of out-of-control processes in fire costs, which could lead to decisions regarding changes in maintenance and repair schedules, repositioning of fire stations, and similar measures.
3. Differentiating Between Fire Dimensions and Costs: For instance, a fire may occur in a dry grassland with relatively low extinguishing costs but, due to its large size, require significant time and human resources. Conversely, a fire confined to a residential unit may not cover extensive dimensions but may incur high costs due to property damage.

In this study, the time between events is assumed to follow an exponential distribution. Its probability density function is given by:

$$f(t,\lambda) = re^{-rt} \quad t \geq 0, \tag{1}$$

When the process is in-control, $r_T = r_0$; otherwise, $r_T = \theta r_0 = r_1$. where θ is the shift parameter for the mean of TBEs.

The event magnitude is modeled as a two-dimensional variable following a bivariate normal distribution. The probability density function of the vector [XY] is equal to:

$$f(x,y)=\frac{1}{2\pi\sigma_X\sigma_Y\sqrt{1-\rho^2}}\exp\left(-\frac{1}{2(1-\rho^2)}\left[\left(\frac{x-\mu_X}{\sigma_X}\right)^2-2\rho\left(\frac{x-\mu_X}{\sigma_X}\right)\left(\frac{Y-\mu_Y}{\sigma_Y}\right)+\left(\frac{Y-\mu_Y}{\sigma_Y}\right)^2\right]\right), \tag{2}$$

Where ρ is the correlation coefficient of X and Y and $\sigma_X > 0$, $\sigma_Y > 0$. Also,

$$\boldsymbol{\mu}_{\mathbf{m}}=\begin{pmatrix}\boldsymbol{\mu}_{\mathbf{X}}\\ \boldsymbol{\mu}_{\mathbf{Y}}\end{pmatrix},$$
$$\boldsymbol{\Sigma}=\begin{pmatrix}\boldsymbol{\sigma}_{\mathbf{X}}^{\mathbf{2}} & \boldsymbol{\rho\sigma}_{\mathbf{X}}\boldsymbol{\sigma}_{\mathbf{Y}}\\ \boldsymbol{\rho\sigma}_{\mathbf{X}}\boldsymbol{\sigma}_{\mathbf{Y}} & \boldsymbol{\sigma}_{\mathbf{Y}}^{\mathbf{2}}\end{pmatrix}, \tag{3}$$

Here, $\boldsymbol{\mu}_{\mathbf{m}}$ represents the mean vector of the magnitude, and $\boldsymbol{\Sigma}$ denotes the covariance matrix of the magnitude. When the process is in-control, the shift parameter θ for the magnitude takes a value greater than 1 ($\theta > 1$), since a value of $\theta < 1$ indicates the process magnitude is in a favorable state.

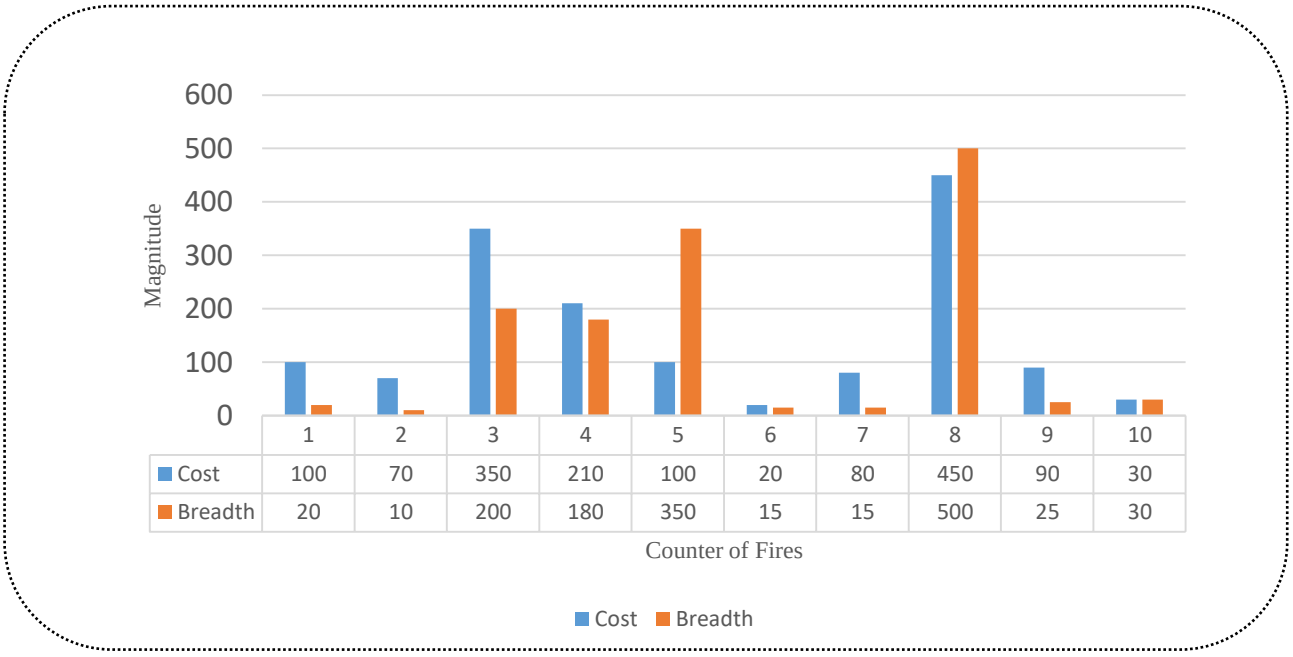

Fig. 1. An example of 10 fires receiving services assuming the TBEs is in-control

III. METHODOLOGY FOR MONITORING

A. Standardization

Since TBEs and each magnitude dimension have different measurement units, standardization is applied to eliminate these differences. This approach enables unified analysis and unbiased monitoring. The magnitude of the cost is represented by X and the magnitude of the extent by Y, where μ_X and μ_Y represent the averages of the in-control condition for X and Y, respectively. Similarly, TBEs are represented by T, with μ_T representing the average of the in-control condition for T. The standardized parameters for monitoring are then $\acute{X}$, $\acute{Y}$ and $\acute{T}$, as follows:

$$\acute{X} = \frac{X}{\mu_X} \ , \quad \acute{Y} = \frac{Y}{\mu_Y} \ , \quad \acute{T} = \frac{T}{\mu_T} \tag{4}$$

B. Implication of the standardized EWMAZ statistic

Consider the three-component (t_i, x_i, y_i) for event counter $(i = 1,2, \dots, n)$ where t_i is the TBE of the event i, x_i is the first dimension of the magnitude and y_i is the second dimension. the following steps must be implemented in order:

1. The first observation E_1occurs, consisting of three components (t_i, x_i, y_i). The time between the two events is determined by defining $T_0 = 0$ as the initial (zero) event, which is assumed to have zero magnitude (representing neither cost nor extent).
2. The event generation process is repeated 5000 times through simulation using Python software, and the values of μ_{T_0}, μ_{X_0}, and μ_{Y_0}, which are used for data standardization, are obtained during this procedure.
3. The next phase of the simulation begins with assigning an initial value to the UCL. In this step, for each generated event, the standardized values $(\acute{T}, \acute{X}, \acute{Y})$ are computed by dividing the observed time or magnitude of the event by the corresponding mean of the in-control process.
4. Then, for each event, the maximum (Max) value of its magnitude is selected using equation (5):

$$M_i = \max\{\acute{X}_i, \acute{Y}_i\} , \tag{5}$$

5. The value of the statistic z_i is obtained using Equation (6):

$$z_i = M_i - \acute{T}_i , \tag{6}$$

Since our goal is to detect out-of-control situations where either the magnitude of events increases or the time between events decreases, the smaller the value of the z_i statistic, the better.

6. The value of the EWMAZ statistic (U_i) is obtained using Equation (7):

$$U_i = (1 - \lambda)U_{i-1} + \lambda(z_i), \tag{7}$$

where $0 < \lambda < 1$ is the smoothing constant, U_{i-1} is the EWMA statistic for previous events, and z_i is the statistic obtained from Equation (6). To increase the detection speed of out-of-control conditions, $(\frac{UCL}{2})$ is replaced in the condition $EWMA - Z_i < 0$.

7. The ARL value is calculated by simulating the $EWMA - Z_i$ statistic 5000 times. This procedure is carried out to achieve $ARL_0 = 200$. Whenever the $EWMA - Z_i$ statistic exceeds the upper control limit, the process is considered out of control, and a signal is triggered. Three different values for the smoothing coefficient are taken into account. The corresponding UCL values for each smoothing coefficient are presented in Table I.

C. Execution of the Three Individual EWMA (TSEWMA)

The three individual EWMA statistics, referred to as TSEWMA, consist of separate EWMA charts—one dedicated to monitoring the time between events, and the other two focused on tracking the magnitude of events. These three statistics operate concurrently to promptly detect any out-of-control conditions.

Given that both the magnitude dimensions and the time between events pertain to undesirable events (where a decrease in magnitude and an increase in TBE are favorable), and since the objective is to identify deviations indicating an out-of-control state, these statistics are monitored with respect to their upper control limits. To achieve $ARL_{0-overall} = 200$, the simulation was implied, and the control limits for three smoothing coefficients of 0.1, 0.5, and 0.9 are considered. Note that the upper control limit for each control chart is set by simulation to obtain ARL_0=600, leading to an overall in-control ARL of 200 for three control charts simultaneously.

The statistics of EWMA-T and EWMA-X and EWMA-Y are defined as follows:

$$a_i = (1-\lambda)a_{i-1} + \lambda(T_i), \tag{8}$$

$$b_i = (1-\lambda)b_{i-1} + \lambda(X_i), \tag{9}$$

$$c_i = (1-\lambda)c_{i-1} + \lambda(Y_i), \tag{10}$$

where $0 < \lambda < 1$ is the smoothing constant, a_i is the EWMA-T statistic for the time between events, and b_i and c_i are the EWMA-X and EWMA-Y statistics for the magnitude data, respectively. $a_0 = b_0 = c_0 = 0$, T_i and X_i and Y_i are TBE and magnitude of events, respectively.

IV. PERFORMANCE COMPARISON

In this section, a numerical example is simulated to assess the performance of the proposed control charts. It is assumed that the time between events (T) follows an exponential distribution with a mean of 2. Additionally, the magnitude of the events is considered to be two-dimensional (*X* and *Y*), following a bivariate normal distribution with means of 10 and 12, respectively, and the following covariance matrix:

$$Q = \begin{bmatrix} 2 & 2 \\ 2 & 3 \end{bmatrix}$$

Here, Q_{11} is the variance of the X, Q_{12} is the covariance of X and Y, Q_{21} is the covariance of *Y* and *X*, and Q_{22} is the variance of *Y*. In this study, the Average Run Length (ARL) criterion is applied at the onset of the shift, starting from the beginning of the monitoring period (zero-state ARL). Through 5000 simulations of the EWMAZ and TSEWMA statistics on the dataset, the Upper Control Limit (UCL) values are determined using the Python programming language. The scope of this study is confined to three smoothing coefficients for each statistic ($\lambda = 0.05,\ \lambda = 0.1,\ \lambda = 0.2$):

Table I. Different smoothing coefficients for statistics and the UCLs

Statistic	UCL for $\lambda = 0.05$	UCL for $\lambda = 0.1$	UCL for $\lambda = 0.2$
EWMAZ	0.297	0.44	0.62
TSEWMA	For TBE: 1.27 For X: 1.033 For Y: 1.033	For TBE: 1.725 For X: 1.084 For Y: 1.086	For TBE: 1.98 For X: 1.109 For Y: 1.111

To evaluate the performance, the parameter θ will be considered as a shift parameter, applied to the mean of time between events (*T*), the first dimension of magnitude (*X*) and the second dimension of magnitude (*Y*). In the following analysis, different shifts will be applied simultaneously to the mean of the time between events and the dimensions of the magnitude. Tables 2 to 7 present the performance of the proposed statistics.

Table II. Average run length under different shift values on the mean of TBE

θ	$\lambda = 0.05$ $UCL_{EWMAZ} = 0.297$	$\lambda = 0.1$ $UCL_{EWMAZ} = 0.44$	$\lambda = 0.2$ $UCL_{EWMAZ} = 0.62$	$\lambda = 0.05$ $UCL_{T-EWMA} = 1.27$ $UCL_{X-EWMA} = 1.033$ $UCL_{Y-EWMA} = 1.033$	$\lambda = 0.1$ $UCL_{T-EWMA} = 1.725$ $UCL_{X-EWMA} = 1.084$ $UCL_{Y-EWMA} = 1.086$	$\lambda = 0.2$ $UCL_{T-EWMA} = 1.98$ $UCL_{X-EWMA} = 1.109$ $UCL_{Y-EWMA} = 1.111$
0.02	7.27	5.91	4.76	163.87	411.82	137.21
0.04	7.43	6.10	4.93	163.22	412.57	137.34
0.06	7.58	6.23	5.09	163.21	411.63	136.90
0.08	7.77	6.38	5.24	160.72	410.24	137.46
0.1	7.96	6.55	5.42	162.87	415.20	138.84
0.12	8.15	6.76	5.63	160.93	415.65	137.24
0.14	8.37	6.93	5.87	162.54	415.33	136.86
0.16	8.61	7.18	6.10	163.30	415.29	137.35
0.18	8.90	7.42	6.35	164.40	394.20	138.01
0.2	9.11	7.65	6.63	165.69	357.83	133.47

As can be seen in Table II, The EWMAZ statistic outperforms the TSEWMA statistic across all three specified smoothing coefficients. The EWMAZ statistic with a smoothing coefficient of 0.1 performs well in detecting shifts in the average time between events across all shift modes. Based on these observations, it can be concluded that the TSEWMA statistic is ineffective in detecting out-of-control situations when the mean time between events changes. Fig. 2 shows an example of 5000 simulation runs under the condition where the shift parameter is $\theta = 0.2$, and the smoothing coefficients for the charts are 0.1, 0.5 and 0.9, respectively. The EWMAZ statistic with a smoothing parameter 0.1 detects the out-of-control situation faster than the others. Factors such as seasonal changes, repeated vandalism, temperature fluctuations, and wind intensity can contribute to a reduction in the time between events.

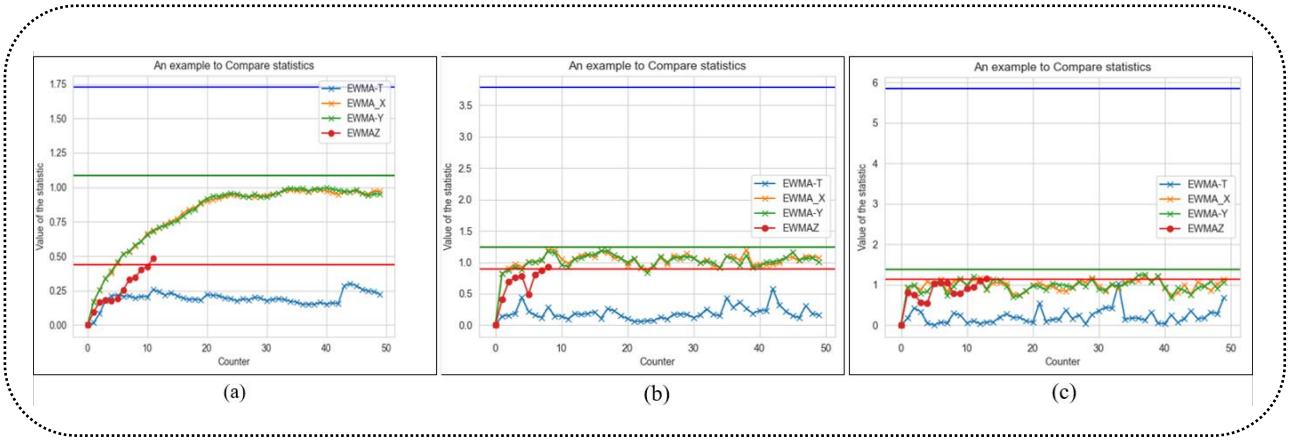

Fig. 2. Comparing the performance of the statistics when the shift occurs on the mean of TBEs.
(a) Smoothing coefficient = 0.1, (b) Smoothing coefficient = 0.5, (c) Smoothing coefficient = 0.9 ($\theta = 0.2$)

Table III. Average run length under different shift values on the mean of X

θ	$\lambda = 0.05$ $UCL_{EWMAZ} = 0.297$	$\lambda = 0.1$ $UCL_{EWMAZ} = 0.44$	$\lambda = 0.2$ $UCL_{EWMAZ} = 0.62$	$\lambda = 0.05$ $UCL_{T-EWMA} = 1.27$ $UCL_{X-EWMA} = 1.033$ $UCL_{Y-EWMA} = 1.033$	$\lambda = 0.1$ $UCL_{T-EWMA} = 1.725$ $UCL_{X-EWMA} = 1.084$ $UCL_{Y-EWMA} = 1.086$	$\lambda = 0.2$ $UCL_{T-EWMA} = 1.98$ $UCL_{X-EWMA} = 1.109$ $UCL_{Y-EWMA} = 1.111$
1.05	138.60	137.38	137.63	70.96	67.11	37.63
1.10	94.85	89.11	92.85	53.10	30.05	19.56
1.15	65.86	62.38	60.72	43.81	26.51	14.04
1.20	48.02	44.79	42.39	37.90	21.75	11.11
1.25	36.63	34.56	30.52	33.63	18.73	9.34
1.30	30.00	26.58	23.53	30.40	16.59	8.16
1.35	24.55	21.76	18.41	27.81	14.92	7.26
1.40	21.17	18.59	15.33	25.68	13.65	6.59
1.45	18.43	15.48	13.24	23.83	12.57	6.03
1.50	16.24	13.46	11.25	22.23	11.74	5.53

In Table III, the TSEWMA statistic generally performs better than the EWMAZ statistic. This superiority is evident across all incremental shifts over the mean of magnitude of the first dimension. The control chart with a smoothing coefficient of 0.9 clearly shows the out-of-control condition faster than other control charts. However, this superiority becomes weaker with the increase in the shift parameter. For example, considering the first dimension as cost (as illustrated in the previous section), factors such as the extent of the fire, the sensitivity and importance of the location, and proximity to residential areas can cause shifts in the mean cost. Fig. 3 presents results from 5,000 simulation runs under conditions where the shift parameter is set to θ = 1.2, with chart smoothing coefficients of 0.1, 0.5, and 0.9, respectively. The TSEWMA statistic detects the out-of-control state faster than other methods across all three smoothing coefficients. Among the three TSEWMA statistics, EWMA-X (shown in yellow in Fig. 3) demonstrates particularly rapid detection of out-of-control situations due to changes in the mean of X.

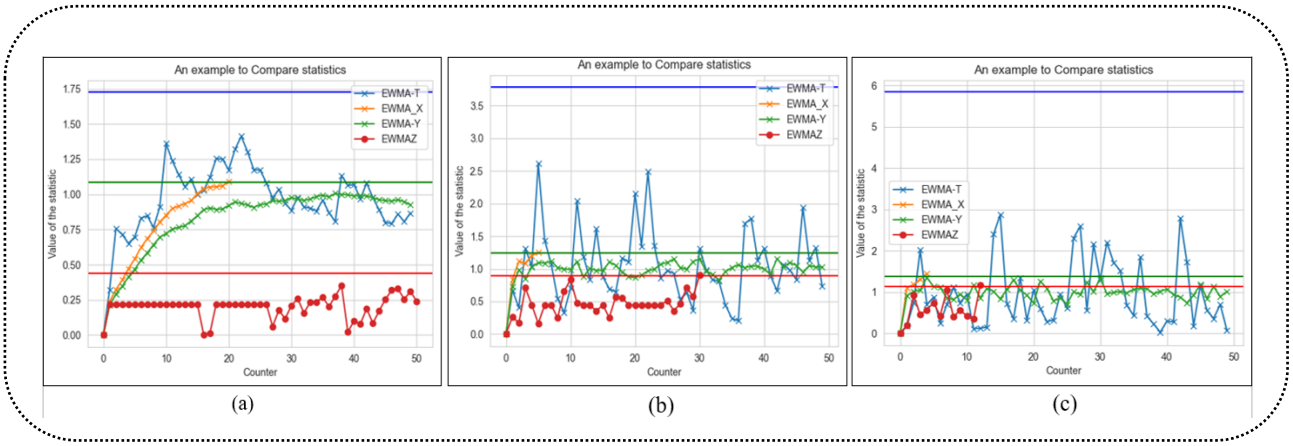

Fig. 3. Comparing the performance of the statistics when shift occurs on the mean of *X*.
(a) Smoothing coefficient = 0.1, (b) Smoothing coefficient = 0.5, (c) Smoothing coefficient = 0.9 ($\theta = 1.2$)

Table IV. Average run length under different shift values on the mean of Y

θ	$\lambda = 0.05$ $UCL_{EWMAZ} = 0.297$	$\lambda = 0.1$ $UCL_{EWMAZ} = 0.44$	$\lambda = 0.2$ $UCL_{EWMAZ} = 0.62$	$\lambda = 0.05$ $UCL_{T-EWMA} = 1.27$ $UCL_{X-EWMA} = 1.033$ $UCL_{Y-EWMA} = 1.033$	$\lambda = 0.1$ $UCL_{T-EWMA} = 1.725$ $UCL_{X-EWMA} = 1.084$ $UCL_{Y-EWMA} = 1.086$	$\lambda = 0.2$ $UCL_{T-EWMA} = 1.98$ $UCL_{X-EWMA} = 1.109$ $UCL_{Y-EWMA} = 1.111$
1.05	140.33	137.70	136.94	71.20	69.07	37.76
1.10	93.27	90.88	89.95	52.72	36.76	20.25
1.15	65.55	61.41	58.00	43.84	26.63	14.22
1.20	40.20	45.37	40.71	37.92	21.94	11.17
1.25	36.66	32.96	29.62	33.59	18.89	9.45
1.30	29.98	26.92	23.21	30.37	16.70	8.21
1.35	24.55	22.07	18.74	27.75	15.11	6.62
1.40	21.16	18.11	16.16	25.63	13.75	6.05
1.45	18.36	15.71	12.94	23.85	12.69	5.38
1.50	16.18	13.70	11.28	22.24	11.72	4.93

Again, in Table IV, the TSEWMA statistic outperforms the EWMAZ statistic. However, when using a smoothing parameter of 0.9, the performance difference between the statistics becomes negligible except at θ = 1.2, where both statistics demonstrate acceptable performance. For example, considering the second dimension as extent, factors such as temperature fluctuations, wind intensity variations, and environmental flammability can cause shifts (changes) in the mean extent. Fig. 4 presents results from 5,000 simulation runs under conditions with a shift parameter of θ = 1.2 and chart smoothing coefficients of 0.1, 0.5, and 0.9. The TSEWMA statistic consistently detects the out-of-control state faster than the other charts across all three smoothing coefficients. Among the three statistics comprising the TSEWMA, the EWMA-Y (depicted in green in Fig. 3) rapidly signals the out-of-control condition due to the change occurring in the mean of *Y*.

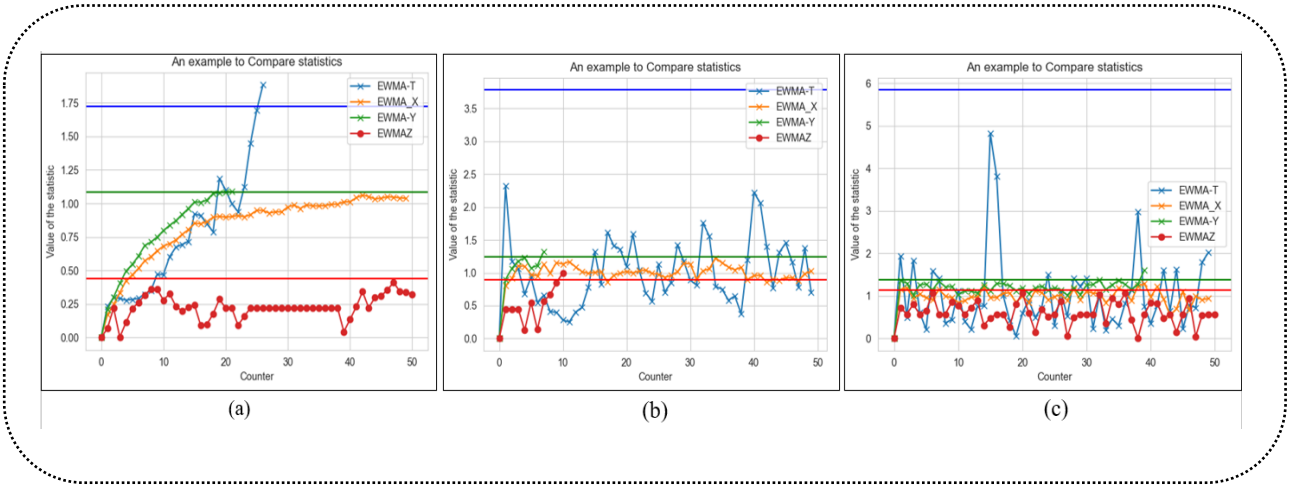

Fig. 4. Comparing the performance of the statistics when shift occurs on the mean of Y.
(a) Smoothing coefficient = 0.1, (b) Smoothing coefficient = 0.5, (c) Smoothing coefficient = 0.9 ($\theta = 1.2$)

In Table V, the time between events is assumed to be in-control while both magnitude dimensions simultaneously confront incremental shifts. As the observations show, the TSEWMA statistic detects out-of-control situations much faster than the EWMAZ statistic. Among all observations, the TSEWMA statistic with a smoothing coefficient of 0.9 shows the best performance. Additionally, this configuration maintains acceptable performance across all shift parameter values except θ = 1.2.. As can be seen in Fig. 5, both statistics show better performance by increasing the smoothing coefficient. For example, with a smoothing coefficient of 0.5, the TSEWMA statistic shows the out-of-control situation at observation 18, while the EWMAZ statistic detects it at observation 24. In contrast, with a smoothing coefficient of 0.9, detection occurs earlier for both statistics: observation 4 for TSEWMA and observation 6 for EWMAZ.

Table VI illustrates a special case where the average time between events undergoes incremental shifts alongside changes in event magnitudes. This condition is favorable for the time between events because the average time increases. Since the events considered in this study are negative events, an increase in the meantime between events is highly satisfactory. The purpose of this case study is to assess the performance of the given control charts under these specific conditions. In this scenario, the TSEWMA statistic demonstrates better performance across all incremental shifts applied to the average parameters of interest. Additionally, Fig. 6 provides an observation of 5000 data points under different smoothing coefficients.

The analysis of Table VI and Fig. 6 allows for insights into the behavior and effectiveness of the control charts in the presence of incremental shifts in the average time between events and their magnitudes. The superior performance of the TSEWMA statistic highlights its suitability for monitoring such conditions. These findings contribute to a deeper understanding of the control chart's performance under specific scenarios and can assist in selecting the most appropriate monitoring approach for similar situations in the future.

Table V. Average run length under different shift values on the average of magnitude X and Y

$\boldsymbol{\theta}$	$\boldsymbol{\lambda = 0.05}$ $\boldsymbol{UCL_{EWMAZ} = 0.297}$	$\boldsymbol{\lambda = 0.1}$ $\boldsymbol{UCL_{EWMAZ} = 0.44}$	$\boldsymbol{\lambda = 0.2}$ $\boldsymbol{UCL_{EWMAZ} = 0.62}$	$\boldsymbol{\lambda = 0.05}$ $\boldsymbol{UCL_{T-EWMA} = 1.27}$ $\boldsymbol{UCL_{X-EWMA} = 1.033}$ $\boldsymbol{UCL_{Y-EWMA} = 1.033}$	$\boldsymbol{\lambda = 0.1}$ $\boldsymbol{UCL_{T-EWMA} = 1.725}$ $\boldsymbol{UCL_{X-EWMA} = 1.084}$ $\boldsymbol{UCL_{Y-EWMA} = 1.086}$	$\boldsymbol{\lambda = 0.2}$ $\boldsymbol{UCL_{T-EWMA} = 1.98}$ $\boldsymbol{UCL_{X-EWMA} = 1.109}$ $\boldsymbol{UCL_{Y-EWMA} = 1.111}$
1.05	116.03	112.36	111.15	67.52	59.79	31.85
1.10	74.99	72.24	68.00	51.54	33.92	18.12
1.15	53.00	48.89	45.98	42.03	25.66	13.21
1.20	39.92	36.50	33.18	37.36	21.25	10.65
1.25	31.74	29.32	25.53	33.21	18.32	9.05
1.30	25.81	23.17	19.97	29.95	16.32	7.94
1.35	22.01	19.20	16.27	27.48	14.74	7.08
1.40	19.05	16.60	13.78	25.33	13.43	6.42
1.45	17.15	14.31	11.64	23.54	12.41	5.88
1.50	14.85	12.55	10.33	22.04	11.56	5.43

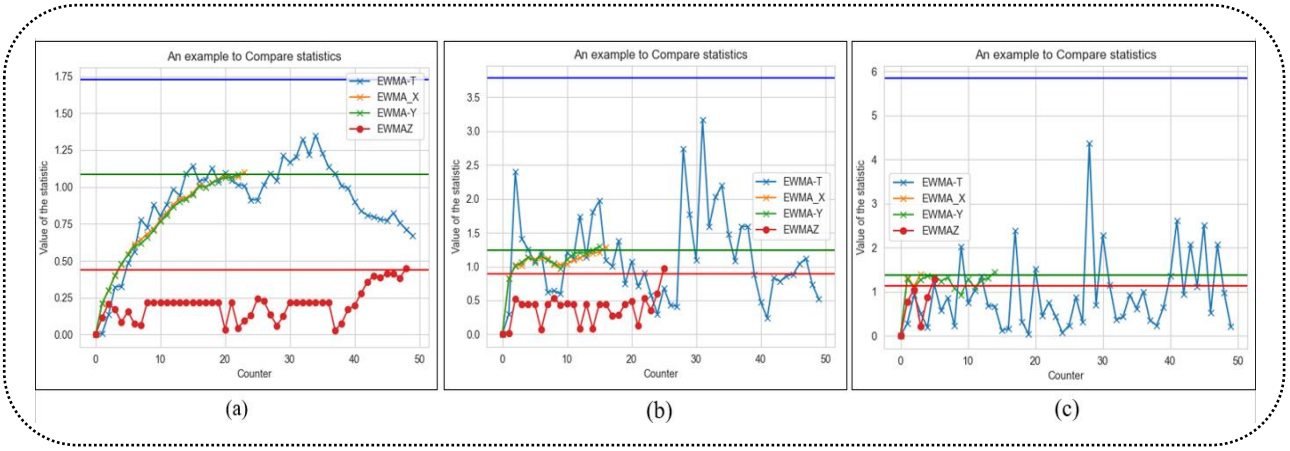

Fig. 5. Comparing the performance of the statistics when shift occurs on the mean of X and Y.
(a) Smoothing coefficient = 0.1, (b) Smoothing coefficient = 0.5, (c) Smoothing coefficient = 0.9 ($\theta = 1.2$)

Table VI. Average run length under different shift values on the average of magnitude X and Y and TBEs

θ	$\lambda = 0.05$ $UCL_{EWMAZ} = 0.297$	$\lambda = 0.1$ $UCL_{EWMAZ} = 0.44$	$\lambda = 0.2$ $UCL_{EWMAZ} = 0.62$	$\lambda = 0.05$ $UCL_{T-EWMA} = 1.27$ $UCL_{X-EWMA} = 1.033$ $UCL_{Y-EWMA} = 1.033$	$\lambda = 0.1$ $UCL_{T-EWMA} = 1.725$ $UCL_{X-EWMA} = 1.084$ $UCL_{Y-EWMA} = 1.086$	$\lambda = 0.2$ $UCL_{T-EWMA} = 1.98$ $UCL_{X-EWMA} = 1.109$ $UCL_{Y-EWMA} = 1.111$
1.02	187.73	179.96	181.45	86.58	122.44	54.42
1.04	172.49	162.01	149.28	70.81	72.09	35.39
1.06	168.73	148.72	134.72	61.11	49.98	26.75
1.08	155.61	136.67	124.97	54.74	39.46	21.17
1.10	145.92	124.38	109.56	49.72	33.66	17.62
1.12	139.65	117.75	100.27	45.82	29.50	15.22
1.14	130.69	110.86	91.56	42.76	26.45	13.56
1.16	129.91	101.23	82.58	40.01	24.21	12.28
1.18	118.49	97.20	77.08	37.83	22.46	11.21
1.20	117.00	89.65	71.38	36.06	20.99	10.45

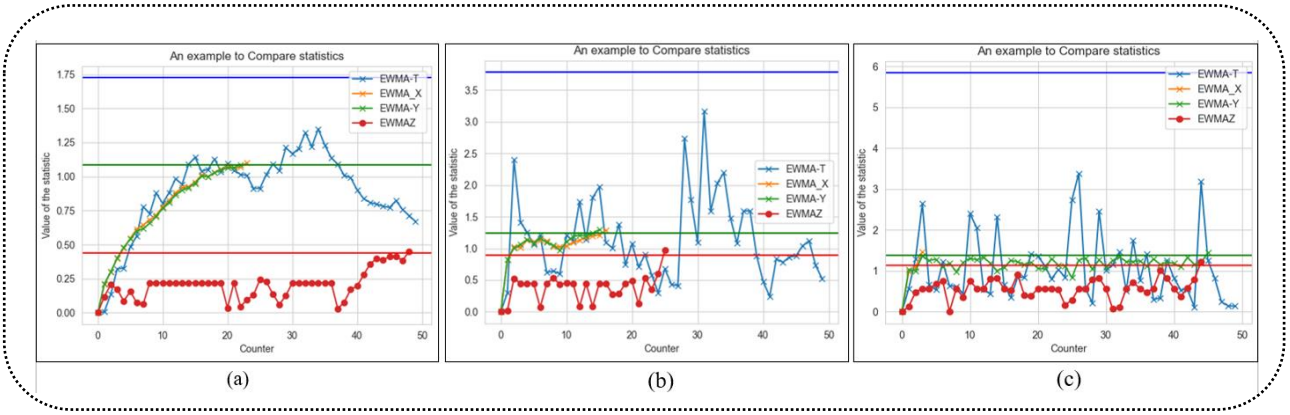

Fig. 6. Comparing the performance of the statistics when shift occurs on the mean of X and Y and TBEs (special case).
(a) Smoothing coefficient = 0.1, (b) Smoothing coefficient = 0.5, (c) Smoothing coefficient = 0.9 ($\theta = 1.2$)

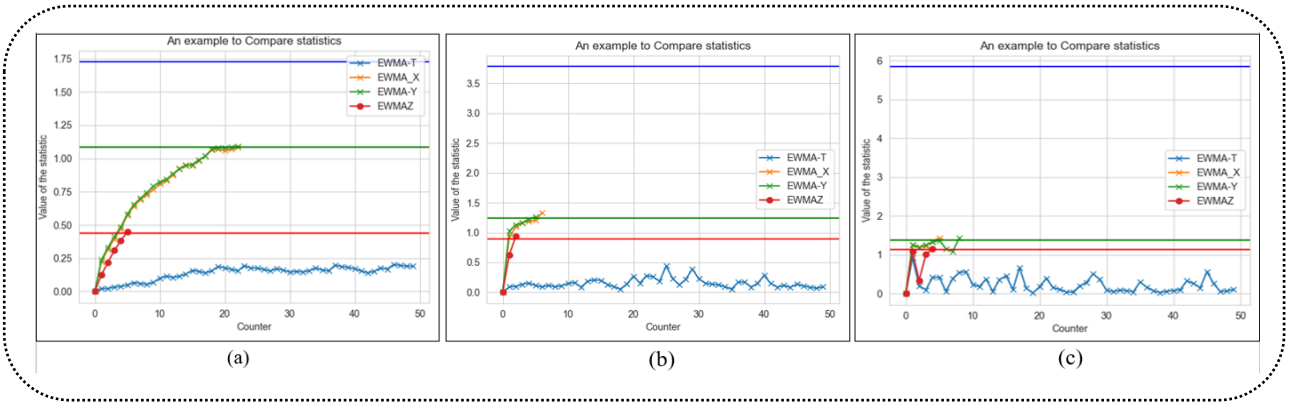

Fig. 7. Comparing the performance of the statistics when shift occurs on the mean of X and Y and TBEs (special case). (a) Smoothing coefficient = 0.1, (b) Smoothing coefficient = 0.5, (c) Smoothing coefficient = 0.9 ($\theta_M = 1.2$ and $\theta_T = 0.2$)

Table VII. Average run length under different shift values on the average of magnitude X without considering Y

θ	$\lambda = 0.05$ $UCL_{EWMAZ} = 0.297$	$\lambda = 0.1$ $UCL_{EWMAZ} = 0.44$	$\lambda = 0.2$ $UCL_{EWMAZ} = 0.62$	$\lambda = 0.05$ $UCL_{T-EWMA} = 1.27$ $UCL_{X-EWMA} = 1.033$ $UCL_{Y-EWMA} = 1.033$	$\lambda = 0.1$ $UCL_{T-EWMA} = 1.725$ $UCL_{X-EWMA} = 1.084$ $UCL_{Y-EWMA} = 1.086$	$\lambda = 0.2$ $UCL_{T-EWMA} = 1.98$ $UCL_{X-EWMA} = 1.109$ $UCL_{Y-EWMA} = 1.111$
1.05	168.27 (116.03)	162.29 (112.36)	169.84 (111.15)	71.10 (67.52)	67.06 (59.79)	37.62 (31.85)
1.10	98.43 (74.99)	96.88 (72.24)	91.82 (68.00)	53.14 (51.54)	35.84 (33.92)	19.82 (18.12)
1.15	67.96 (53.00)	64.80 (48.89)	59.89 (45.98)	43.83 (42.03)	26.55 (25.66)	13.91 (13.21)
1.20	47.67 (39.92)	44.15 (36.50)	40.90 (33.18)	37.91 (37.36)	21.80 (21.25)	11.16 (10.65)
1.25	37.30 (31.74)	33.94 (29.32)	30.79 (25.53)	33.64 (33.21)	18.73 (18.32)	9.42 (9.05)
1.30	29.93 (25.81)	26.62 (23.17)	22.95 (19.97)	30.39 (29.95)	16.62 (16.32)	8.16 (7.94)
1.35	25.21 (22.01)	21.79 (19.20)	18.47 (16.27)	27.73 (27.48)	15.02 (14.74)	7.31 (7.08)
1.40	20.75 (19.05)	18.05 (16.60)	15.32 (13.78)	25.63 (25.33)	13.65 (13.43)	6.59 (6.42)
1.45	18.48 (17.15)	15.75 (14.31)	12.98 (11.64)	23.80 (23.54)	12.61 (12.41)	6.03 (5.88)
1.50	16.27 (14.85)	13.72 (12.55)	11.21 (10.33)	22.28 (22.04)	11.71 (11.56)	5.57 (5.43)

Table VII presents the worst-case scenario for shift occurrences. It examines the mean of the time between events for decreasing shifts and the mean of the event magnitude for increasing shifts. This scenario is considered the worst due to the negativity of the event types. From the table, it can be observed that both statistics perform well in detecting out-of-control states. However, the TSEWMA statistic shows weakness when the shifts related to the magnitude remain constant while the shifts related to the time between events change. Thus, it can be concluded that the TSEWMA statistic is effective in detecting changes in the average magnitude of events but is inefficient in detecting shifts in the time between events.

Based on the observations from the presented tables and figures, it is evident that both the EWMAZ and TSEWMA statistics can be utilized in situations where the magnitude of events has multiple dimensions and simultaneous monitoring of these dimensions along with the time between events is desired. Although the TSEWMA statistic outperforms the EWMAZ statistic when the magnitude of events changes, it lacks acceptable performance in detecting simultaneous changes. Therefore, the following conclusions can be drawn:

1. The EWMAZ statistic should be employed when the simultaneous monitoring of the time between events and event magnitude is prioritized without emphasizing one over the other.
2. The EWMAZ statistic is suitable for prioritizing the monitoring of the time between events in a simultaneous monitoring scenario.
3. The TSEWMA statistic should be used when the priority is to monitor the magnitude of events.

These conclusions are based on the observed performance of the statistics, taking into account different monitoring priorities. By selecting the appropriate statistic based on the specific monitoring needs, more effective and efficient control can be achieved.

Table VIII. Average run length under different shift values on the average of magnitude X and Y and TBEs

θ_M	θ_T	$\lambda = 0.05$ $UCL_{EWMAZ} = 0.297$	$\lambda = 0.1$ $UCL_{EWMAZ} = 0.44$	$\lambda = 0.2$ $UCL_{EWMAZ} = 0.62$	$\lambda = 0.05$ $UCL_{T-EWMA} = 1.27$ $UCL_{X-EWMA} = 1.033$ $UCL_{Y-EWMA} = 1.033$	$\lambda = 0.1$ $UCL_{T-EWMA} = 1.725$ $UCL_{X-EWMA} = 1.084$ $UCL_{Y-EWMA} = 1.086$	$\lambda = 0.2$ $UCL_{T-EWMA} = 1.98$ $UCL_{X-EWMA} = 1.109$ $UCL_{Y-EWMA} = 1.111$
1.05	1.01	123.28	119.79	116.64	67.72	59.12	31.55
	1.02	131.65	130.12	122.67	66.52	58.69	31.18
	1.03	139.83	135.86	131.81	66.68	57.63	31.06
	1.04	151.83	142.16	138.96	66.35	58.86	30.39
	1.05	170.80	151.22	143.93	65.84	57.81	30.68
1.10	1.01	79.17	75.16	72.93	51.39	33.78	18.16
	1.02	83.01	75.79	74.07	51.21	33.67	18.07
	1.03	87.70	84.33	80.17	51.53	33.56	18.00
	1.04	97.61	88.16	82.58	50.91	33.45	17.78
	1.05	104.31	95.82	87.77	50.89	33.48	18.01
1.15	1.01	54.63	52.48	48.02	42.82	25.58	13.20
	1.02	58.06	55.89	52.12	42.83	25.56	13.10
	1.03	62.10	57.63	51.86	42.77	25.42	13.11
	1.04	64.37	62.10	53.87	42.53	25.45	13.08
	1.05	68.08	63.36	56.25	42.58	25.35	13.22
1.20	1.01	41.64	36.75	34.65	37.24	21.14	10.61
	1.02	42.99	41.34	36.36	37.23	21.16	10.63
	1.03	44.82	43.06	37.20	37.19	21.07	10.67
	1.04	47.93	43.86	38.25	37.27	21.06	10.61
	1.05	49.41	42.23	40.26	37.10	21.17	10.54

V. COMPARATIVE STUDY

This section considers a scenario where the time between events (TBE) is unidimensional, while the event's magnitude is bidimensional. Traditional control charts are limited in their monitoring capability, as they can only track one of the two magnitude dimensions independently. This limitation arises from the fact that, prior to this research, no multivariate control chart has been introduced to monitor events with a magnitude extending beyond a single dimension.

Table IX. Average run length of the existing control charts (TBE-EWMA & X-EWMA) and proposed control charts under shifts in both magnitude components

θ	$\lambda = 0.05$ $UCL_{TBE-EWMA} = 0.978$ $UCL_{X-EWMA} = 0.774$	$\lambda = 0.2$ $UCL_{TBE-EWMA} = 0.978$ $UCL_{X-EWMA} = 0.774$	$\lambda = 0.05$ $UCL_{EWMAZ} = 0.297$	$\lambda = 0.2$ $UCL_{EWMAZ} = 0.62$	$\lambda = 0.05$ $UCL_{T-EWMA} = 1.27$ $UCL_{X-EWMA} = 1.033$ $UCL_{Y-EWMA} = 1.033$	$\lambda = 0.2$ $UCL_{T-EWMA} = 1.98$ $UCL_{X-EWMA} = 1.109$ $UCL_{Y-EWMA} = 1.111$
1.05	166.79	153.35	116.03	111.15	67.52	31.85
1.10	148.58	150.24	74.99	68.00	51.54	18.12
1.15	144.57	139.01	53.00	45.98	42.03	13.21
1.20	137.37	125.36	39.92	33.18	37.36	10.65
1.25	115.86	109.52	31.74	25.53	33.21	9.05
1.30	102.57	91.34	25.81	19.97	29.95	7.94
1.35	89.88	73.47	22.01	16.27	27.48	7.08
1.40	75.52	64.54	19.05	13.78	25.33	6.42
1.45	63.82	49.85	17.15	11.64	23.54	5.88
1.50	50.30	28.74	14.85	10.33	22.04	5.43

This study addresses this gap in the literature by introducing a novel process monitoring approach. Tables 9, 10, and 11 present out-of-control average run length (ARL) values for scenarios where shifts are applied to both magnitude parameters. The two leftmost columns in the comparison tables represent existing control charts, while the remaining four columns correspond to the proposed statistics. Notably, only two smoothing parameters were considered to avoid redundancy.

- Table IX considers a scenario where both magnitude dimensions undergo shifts. No existing chart in the literature simultaneously monitors multivariate time between events and their multivariate magnitudes. Therefore, univariate time between events and magnitude charts, which are commonly used, have been employed. Two charts - one for univariate time between events and another for event magnitude - have been developed based on the characteristics of the normal distribution, as presented in the previous section for the (*X*) component. Consequently, these proposed charts are referred to as the TBE-EWMA (for monitoring TBEs) and X-EWMA (for monitoring component *X* of magnitude) charts. The results clearly demonstrate superior performance of the proposed control charts across all shifts.
- Table X examines a scenario where both magnitude dimensions again undergo shifts. This table employs a univariate time between events and magnitude chart based on the magnitude component *Y*, using the mean and variance defined in the previous section. Thus, two EWMA statistics are implemented: one for TBEs (TBE-EWMA) and another for the magnitude component *Y* (Y-EWMA). The results confirm that univariate monitoring is ineffective compared to the proposed statistics.
- Table XI presents results when shifts are applied to the time between events as well as both magnitude components. For comparison, the TBE-EWMA and Y-EWMA statistics are used alongside the two proposed statistics, each based on different smoothing parameters. Notably, the proposed control charts yield considerably lower ARL values, demonstrating their effectiveness. Furthermore, the statistics for all three smoothing coefficients consistently outperform those found in the literature.

Table X. Average run length of the existing control charts (TBE-EWMA & Y-EWMA) and proposed control charts under shifts in both magnitude components

θ	$\lambda = 0.05$ $UCL_{TBE-EWMA} = 0.976$ $UCL_{Y-EWMA} = 0.771$	$\lambda = 0.2$ $UCL_{TBE-EWMA} = 1.61$ $UCL_{Y-EWMA} = 0.99$	$\lambda = 0.05$ $UCL_{EWMAZ} = 0.297$	$\lambda = 0.2$ $UCL_{EWMAZ} = 0.62$	$\lambda = 0.05$ $UCL_{T-EWMA} = 1.27$ $UCL_{X-EWMA} = 1.033$ $UCL_{Y-EWMA} = 1.033$	$\lambda = 0.2$ $UCL_{T-EWMA} = 1.98$ $UCL_{X-EWMA} = 1.109$ $UCL_{Y-EWMA} = 1.111$
1.05	103.45	77.85	116.03	111.15	67.52	31.85
1.10	98.66	70.14	74.99	68.00	51.54	18.12
1.15	93.75	65.82	53.00	45.98	42.03	13.21
1.20	80.49	58.72	39.92	33.18	37.36	10.65
1.25	73.95	51.13	31.74	25.53	33.21	9.05
1.30	68.24	39.73	25.81	19.97	29.95	7.94
1.35	60.01	30.25	22.01	16.27	27.48	7.08
1.40	57.38	26.82	19.05	13.78	25.33	6.42
1.45	44.42	20.63	17.15	11.64	23.54	5.88
1.50	40.57	18.38	14.85	10.33	22.04	5.43

Table XI. Average run length of the existing control charts (TBE-EWMA & Y-EWMA) and proposed control charts under shifts in both magnitude components and TBEs

θ	$\lambda = 0.05$ $UCL_{TBE-EWMA} = 0.976$ $UCL_{Y-EWMA} = 0.771$	$\lambda = 0.2$ $UCL_{TBE-EWMA} = 1.61$ $UCL_{Y-EWMA} = 0.99$	$\lambda = 0.05$ $UCL_{EWMAZ} = 0.297$	$\lambda = 0.2$ $UCL_{EWMAZ} = 0.62$	$\lambda = 0.05$ $UCL_{T-EWMA} = 1.27$ $UCL_{X-EWMA} = 1.033$ $UCL_{Y-EWMA} = 1.033$	$\lambda = 0.2$ $UCL_{T-EWMA} = 1.98$ $UCL_{X-EWMA} = 1.109$ $UCL_{Y-EWMA} = 1.111$
1.05	137.85	94.76	187.73	181.45	86.58	54.42
1.10	123.28	87.42	172.49	149.28	70.81	35.39
1.15	112.94	77.74	168.73	134.72	61.11	26.75
1.20	101.02	63.85	155.61	124.97	54.74	21.17
1.25	92.75	52.52	145.92	109.56	49.72	17.62
1.30	90.24	40.24	139.65	100.27	45.82	15.22
1.35	83.45	35.95	130.69	91.56	42.76	13.56
1.40	66.93	29.63	129.91	82.58	40.01	12.28
1.45	49.59	20.86	118.49	77.08	37.83	11.21
1.50	39.46	18.48	117.00	71.38	36.06	10.45

VI. CONCLUSION AND SUGGESTIONS FOR FUTURE RESEARCH

This study presented the simultaneous monitoring of the time between events and the magnitude of events when the magnitude has multiple components. While previous studies have discussed monitoring the time between events and their magnitude, there is still a need to consider situations where the magnitude of events has multiple components. Taking a multi-dimensional perspective of event magnitude can enhance monitoring effectiveness and enable the monitoring of processes with multiple dimensions in real-world scenarios. In this research, two EWMA-based statistics were analyzed: the Shewhart-EWMA statistic and the TSEWMA statistic, which combines three single EWMA statistics. Based on the observations, each of these statistics was determined to effectively monitor specific conditions and processes with multi-dimensional magnitude. Continuing research in this field can involve examining complex processes where both the magnitude of events and the timing of events have multiple dimensions. This expanded analysis would provide valuable insights into monitoring techniques for such complex systems. Furthermore, future

research can explore the development of advanced statistical methodologies and algorithms to handle challenges in monitoring multi-dimensional event magnitude and time. Additionally, investigating the integration of other data sources (e.g., contextual information or external factors) into the monitoring process can enhance the accuracy and predictive capabilities of monitoring systems. Overall, the current study provides a foundation for future research on simultaneous monitoring of event timing and multi-dimensional magnitudes. Addressing these research gaps can advance the field of quality control and provide practical solutions for monitoring processes across various industries.

REFERENCES

Abubakar, S. S., Khoo, M. B., Saha, S., & Lee, M. H. (2021). A new exponentially weighted moving average chart with an adaptive control scheme for high yield processes—An application in injection molding process. *Quality and Reliability Engineering International*, *37*(2), 527-540.

Albers, W., & Kallenberg, W. C. (2006). Alternative Shewhart-type charts for grouped observations. *Metron*, *64*(3), 357-375.

Ali, S. (2021). First passage time control charts assuming power law intensity for time to jointly monitor time and magnitude. *Quality and Reliability Engineering International*, *37*(5), 2034-2064.

Ali, S., Zafar, T., Shah, I., & Wang, L. (2020). Cumulative Conforming Control Chart Assuming Discrete Weibull Distribution. *IEEE Access*, *8*, 10123-10133.

Amiri, A., Sogandi, F., & Ayoubi, M. (2018). Simultaneous monitoring of correlated multivariate linear and GLM regression profiles in Phase II. Quality Technology & Quantitative Management, 15(4), 435-458.

Amjadi, N., & Sabri-Laghaie, K. (2022). Median-rate control chart for simultaneous monitoring of frequency and magnitude of events. *Quality and Reliability Engineering International*, *38*(1), 89-109.

Aslam, M., Khan, N., Azam, M., & Jun, C. H. (2014). Designing of a new monitoring t-chart using repetitive sampling. *Information sciences*, *269*, 210-216.

Calvin, T. (1983). Quality control techniques for "zero defects". *IEEE Transactions on Components, Hybrids, and Manufacturing Technology*, *6*(3), 323-328.

Chen, Y. K., & Chen, C. Y. (2012). Cumulative Conformance Count Charts with VariableSample Sizes. *International Journal of Trade, Economics and Finance*, *3*(3), 187-193.

Chen, Y. K., & Chiu, F. R. (2023). AX/T Control Chart-Based CBM Model for Service Facility Maintenance. *Arabian Journal for Science and Engineering*, *48*(5), 7207-722.

Di Bucchianico, A., Mooiweer, G. D., & Moonen, E. J. G. (2005). Monitoring infrequent failures of high-volume production processes. *Quality and Reliability Engineering International*, *21*(5), 521-528.

Dogu, E., & Noor-ul-Amin, M. (2021). Monitoring exponentially distributed time between events data: self-starting perspective. *Communications in Statistics-Simulation and Computation*, 1-13.

Goh, T. N. (1987). A control chart for very high yield processes. *Quality Assurance*, *13*(1), 18-22.

Guo, B., Yang, Y., & Castagliola, P. (2024). Optimal design of time-between-event control charts with parameter estimation. *Quality Engineering*, 1-12.

Hakimia, A., Farughi, H., Amiri, A., & Arkata, J. (2022). Data Consumption Analysis by Two Ordinal Multivariate Control Charts. *International Journal of Engineering*, 35(11),2196-2204.

He, B., Xie, M., Goh, T. N., & Tsui, K. L. (2006). On control charts based on the generalized Poisson model. *Quality Technology & Quantitative Management*, 3(4), 383-400.

He, Y., Mi, K., & Wu, C. (2012). A New Statistical High-Quality Process Monitoring Method: The Counted Number Between Omega-Event Control Charts. *Quality and Reliability Engineering International*, *28*(4), 427-436.

Hu, X., Castagliola, P., Zhong, J., Tang, A., & Qiao, Y. (2021). On the performance of the adaptive EWMA chart for monitoring time between events. *Journal of Statistical Computation and Simulation*, *91*(6), 1175-1211.

Hu, X., Xia, F., Zhang, J., & Song, Z. (2024). Combined Shewhart–EWMA and Shewhart–CUSUM monitoring schemes for time between events. *Quality and Reliability Engineering International*, *40*(6), 3352-3380.

Janada, K., Soltan, H., Hussein, M. S., & Abdel-Shafi, A. (2022). Angular Control Charts: A new perspective for monitoring reliability of multi-state systems. *Computers & Industrial Engineering*, *172*, 108621.

Kumar, N., Rakitzis, A. C., Chakraborti, S., & Singh, T. (2024). Statistical design of ATS-unbiased charts with runs rules for monitoring exponential time between events. *Communications in Statistics-Theory and Methods*, *53*(3), 815-833.

Lucas, J. M. (1985). Counted data CUSUM's. *Technometrics*, *27*(2), 129-144.

Maleki, M. R., Ghashghaei, R., & Amiri, A. (2016). Simultaneous Monitoring of Multivariate Process Mean and Variability in the Presence of Measurement Error with Linearly Increasing Variance under Additive Covariate Model (RESEARCH NOTE). *International Journal of Engineering*, *29*(4), 514-523.

Mirzaei Novin, M., & Amiri, A. (2023). Simultaneous monitoring of multivariate time between events and their magnitude using multivariate marked Hawkes point process. *Quality Technology & Quantitative Management*, 21(6), 1004-1024.

Niaz, A., Khan, M., & Ijaz, M. (2025). One-Sided Modified EWMA Control Charts for Monitoring Time Between Events. *Quality and Reliability Engineering International*.

Pu, W., & Li, Y. (2023). Evaluating structural failure probability during aftershocks based on spatiotemporal simulation of the regional earthquake sequence. *Engineering Structures*, *275*, 115267.

Qu, L., Wu, Z., Khoo, M. B., & Rahim, A. (2014). Time-between-event control charts for sampling inspection. *Technometrics*, *56*(3), 336-346.

Rahali, D., Castagliola, P., Taleb, H., & Khoo, M. B. (2019). Evaluation of Shewhart time-between-events-and-amplitude control charts for several distributions. *Quality Engineering*, *31*(2), 240-254.

Rahali, D., Castagliola, P., Taleb, H., & Khoo, M. B. C. (2021). Evaluation of Shewhart time-between-events-and-amplitude control charts for correlated data. *Quality and Reliability Engineering International*, *37*(1), 219-241

Sanusi, R. A., Teh, S. Y., & Khoo, M. B. (2020). Simultaneous monitoring of magnitude and time-between-events data with a Max-EWMA control chart. *Computers & Industrial Engineering*, *142*, 106378.

Shamstabar, Y., Shahriari, H., & Samimi, Y. (2021). Reliability monitoring of systems with cumulative shock-based deterioration process. *Reliability Engineering & System Safety*, *216*, 107937.

Talib, A., Ali, S., & Shah, I. (2024). Max-EWMA chart for time and magnitude monitoring using generalized exponential distribution. *Communications in Statistics - Simulation and Computation*, *53*(4), 1857–1872.

Vardeman, S., & Ray, D. O. (1985). Average run lengths for CUSUM schemes when observations are exponentially distributed. *Technometrics*, *27*(2), 145-150.

Wu, Z., Khoo, M. B., Shu, L., & Jiang, W. (2009a). An np control chart for monitoring the mean of a variable based on an attribute inspection. *International Journal of Production Economics*, *121*(1), 141-147.

Wu, Z., Jiao, J., & He, Z. (2009b). A control scheme for monitoring the frequency and magnitude of an event. *International Journal of Production Research*, *47*(11), 2887-2902.

Xie, M., Goh, T. N., Kuralmani, V., & Kuralmani, V. (2002). *Statistical models and control charts for high-quality processes*. Springer Science & Business Media.

Zwetsloot, I. M., Mahmood, T., & Woodall, W. H. (2020). Multivariate time-between-events monitoring: An overview and some overlooked underlying complexities. *Quality Engineering*, *33*(1), 13-25.

Zwetsloot, I. M., Mahmood, T., Taiwo, F. M., & Wang, Z. (2023). A real-time monitoring approach for bivariate event data. *Applied Stochastic Models in Business and Industry*, *39*(6), 789-817.